

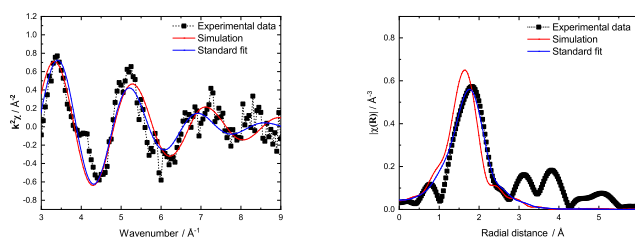
Cite this: DOI: 00.0000/xxxxxxxxxx

## Electronic Supporting Information for: Examination of the short-range structure of molten salts: ThF<sub>4</sub>, UF<sub>4</sub>, and related alkali actinide fluoride systems

J.A. Ocádiz-Flores,<sup>a</sup> A.E. Gheribi,<sup>b†</sup>, J. Vlieland<sup>a</sup>, D. de Haas<sup>a</sup>, K. Dardenne<sup>c</sup>, J. Rothe<sup>c</sup>, R.J.M Konings<sup>a,d</sup>, A.L. Smith<sup>\*a</sup>

### 1 Coordination environment of the actinide cations

Herein are the EXAFS measurements carried out in the molten state for seven different alkali actinide fluoride systems at a few representative compositions. Accompanying the experimental data are the simulated EXAFS oscillations, generated using molecular dynamics (MD) positions as input and those via fitting of the standard EXAFS equations. The Fourier Transform moduli of the signals are shown alongside the EXAFS oscillations (Figs. 1 to 12).



(a) (b)

Fig. 1 (a)Experimental (■), simulated (red), and fitted (blue)  $k^2\chi(k)$  oscillations of (LiF:ThF<sub>4</sub>) = (0.90:0.10) (fluorescence, T = 1133 K, data from<sup>1</sup>). (b) Fourier transform modulus  $|\chi(R)|$  of the EXAFS spectra.

<sup>a</sup> Delft University of Technology, Faculty of Applied Sciences, Radiation Science & Technology Department, Mekelweg 15, 2629 JB Delft, The Netherlands

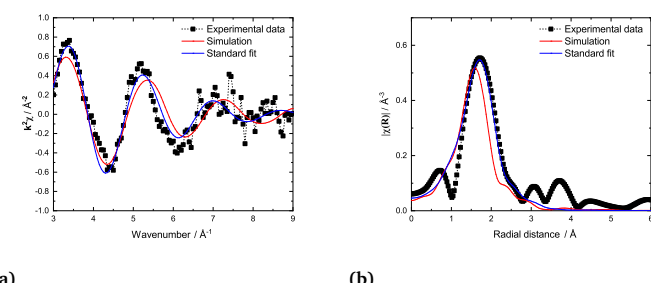
<sup>b</sup> Centre for Research in Computational Thermochemistry, Department of Chemical Engineering, École Polytechnique, C.P. 6079, Succursale "Downtown", Montreal (Quebec), Canada H3C 3A7

<sup>c</sup> Karlsruhe Institute of Technology (KIT), Institute for Nuclear Waste Disposal (INE), Radionuclide Speciation Department, Hermann-von-Helmholtz-Platz 1, 76344 Eggenstein-Leopoldshafen, Germany

<sup>d</sup> European Commission, Joint Research Centre, P.O. Box 2340, D-76125 Karlsruhe, Germany

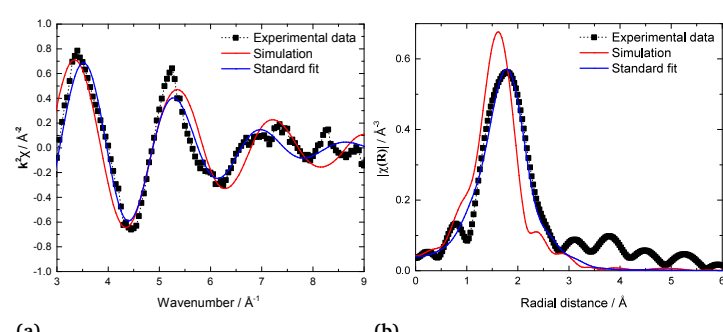
\* E-mail: A.L.Smith@tudelft.nl

† Electronic Supplementary Information (ESI) available: [details of any supplementary information available should be included here]. See DOI: 10.1039/cXCP00000x/



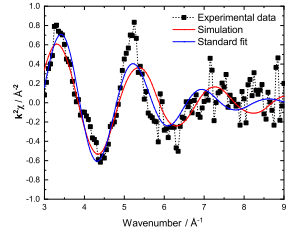
(a) (b)

Fig. 2 (a)Experimental (■), simulated (red), and fitted (blue)  $k^2\chi(k)$  oscillations of (LiF:ThF<sub>4</sub>) = (0.50:0.50) (fluorescence, T = 1193 K, data from<sup>1</sup>). (b) Fourier transform modulus  $|\chi(R)|$  of the EXAFS spectra.

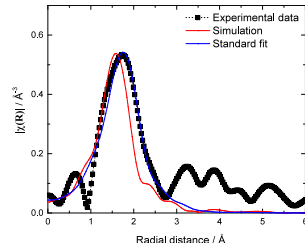


(a) (b)

Fig. 3 (a)Experimental (■), simulated (red), and fitted (blue)  $k^2\chi(k)$  oscillations of (NaF:ThF<sub>4</sub>) = (0.67:0.33) (data taken from<sup>1</sup>, T = 1073 K measured in absorption). (b) Fourier transform modulus  $|\chi(R)|$  of the EXAFS spectra.

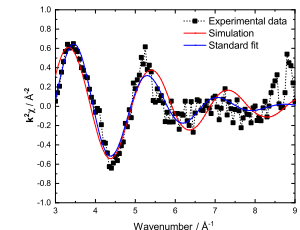


(a)

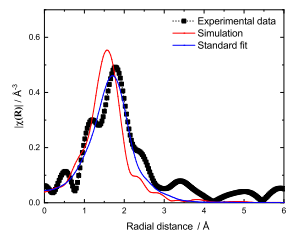


(b)

**Fig. 4** (a)Experimental (■), simulated (red), and fitted (blue)  $k^2\chi(k)$  oscillations of  $(\text{NaF:ThF}_4) = (0.50:0.50)$  (fluorescence, data taken from<sup>1</sup>,  $T= 1108 \text{ K}$ ). (b) Fourier transform modulus  $|\chi(R)|$  of the EXAFS spectra.

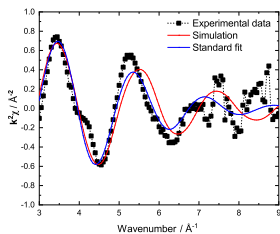


(a)

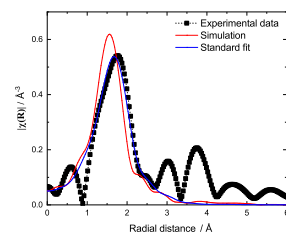


(b)

**Fig. 7** (a)Experimental (■), simulated (red), and fitted (blue)  $k^2\chi(k)$  oscillations of  $(\text{KF:ThF}_4) = (0.50:0.50)$  (fluorescence,  $T= 1209 \text{ K}$ ). (b) Fourier transform modulus  $|\chi(R)|$  of the EXAFS spectra.

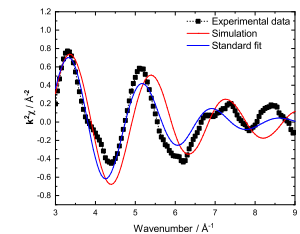


(a)

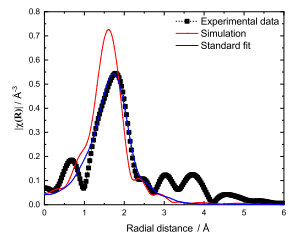


(b)

**Fig. 5** (a)Experimental (■), simulated (red), and fitted (blue)  $k^2\chi(k)$  oscillations of  $(\text{NaF:UF}_4) = (0.50:0.50)$  (absorption,  $T= 1033 \text{ K}$ ). (b) Fourier transform modulus  $|\chi(R)|$  of the EXAFS spectra.

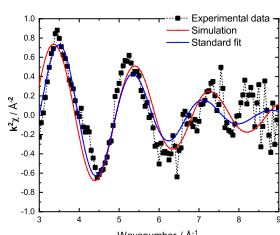


(a)

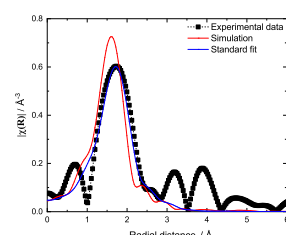


(b)

**Fig. 8** (a)Experimental (■), simulated (red), and fitted (blue)  $k^2\chi(k)$  oscillations of  $(\text{KF:ThF}_4) = (0.33:0.67)$  (absorption,  $T= 1266 \text{ K}$ ). (b) Fourier transform modulus  $|\chi(R)|$  of the EXAFS spectra.

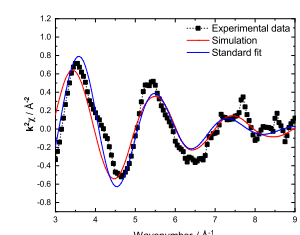


(a)

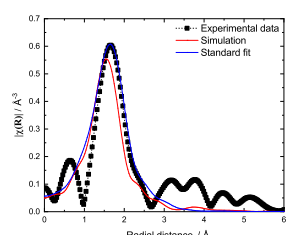


(b)

**Fig. 6** (a)Experimental (■), simulated (red), and fitted (blue)  $k^2\chi(k)$  oscillations of  $(\text{KF:ThF}_4) = (0.833:0.167)$  (fluorescence,  $T= 1060 \text{ K}$ ). (b) Fourier transform modulus  $|\chi(R)|$  of the EXAFS spectra.

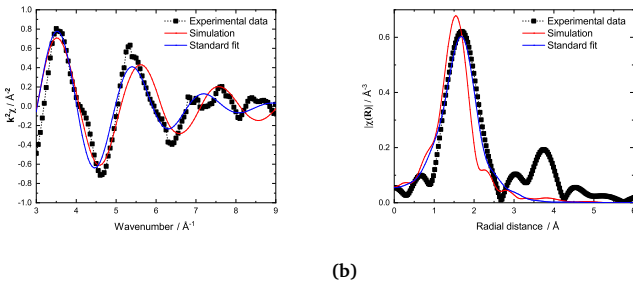


(a)



(b)

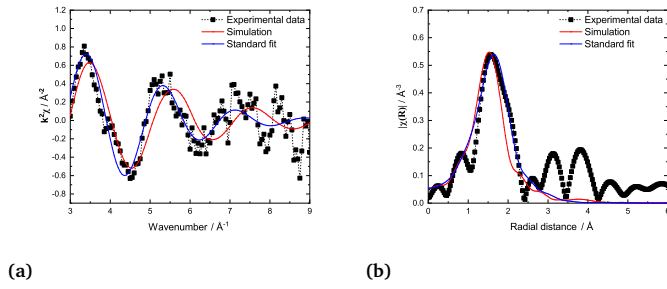
**Fig. 9** (a)Experimental (■), simulated (red), and fitted (blue)  $k^2\chi(k)$  oscillations of  $(\text{KF:UF}_4) = (0.33:0.67)$  (absorption,  $T= 1090 \text{ K}$ ). (b) Fourier transform modulus  $|\chi(R)|$  of the EXAFS spectra.



(a)

(b)

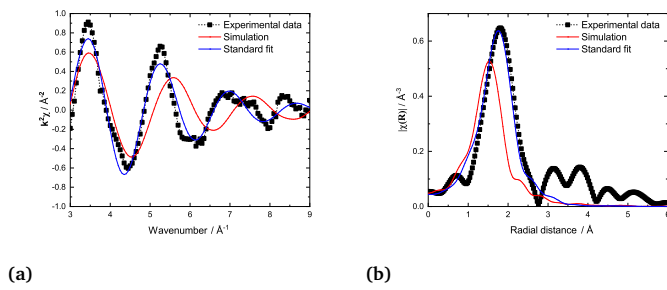
**Fig. 10** (a)Experimental (■), simulated (red), and fitted (blue)  $k^2\chi(k)$  oscillations of  $(\text{CsF:UF}_4) = (0.50:0.50)$  (absorption,  $T = 1058$  K). (b) Fourier transform modulus  $|\chi(R)|$  of the EXAFS spectra.



(a)

(b)

**Fig. 11** (a)Experimental (■), simulated (red), and fitted (blue)  $k^2\chi(k)$  oscillations of  $(\text{CsF:UF}_4) = (0.33:0.67)$  (fluorescence,  $T = 1191$  K). (b) Fourier transform modulus  $|\chi(R)|$  of the EXAFS spectra.



(a)

(b)

**Fig. 12** (a)Experimental (■), simulated (red), and fitted (blue)  $k^2\chi(k)$  oscillations of  $(\text{CsF:ThF}_4) = (0.50:0.50)$  (absorption,  $T = 1201$  K). (b) Fourier transform modulus  $|\chi(R)|$  of the EXAFS spectra.

## 2 Radial distribution functions of the liquid mixtures

The An-F, An-An, and A-F RDFs have been plotted for the three most representative compositions:  $X(\text{AnF}_4) = 0.25$  along with 0.33, 0.50, and 0.67 in Figs. 13–15.

## 3 XANES data

Both Th and U remained in the tetravalent oxidation state as revealed by the XANES data. Uranium in particular is problematic, as it has several valence states and may oxidize when exposed to

the synchrotron beam, whereas Th may be expected to oxidize only as Th(IV). XANES data of uranium-bearing samples in this work are compared to data of uranium samples in three oxidation states:  $\text{UO}_2$  (U(IV)), schoepite (hydrated  $\text{UO}_3$ , U(VI)),  $\text{U}_3\text{O}_8$  (U(V)/U(VI)), measured at the same beamline with a metallic yttrium reference, taken from Kegler et al.<sup>2</sup> and Böhler et al.<sup>3</sup>.  $\text{UO}_2$ , used as a reference for  $\text{UF}_4$  at room temperature in this work, is also included. The energy positions of the inflection points and of the white lines are tabulated in Table 1.

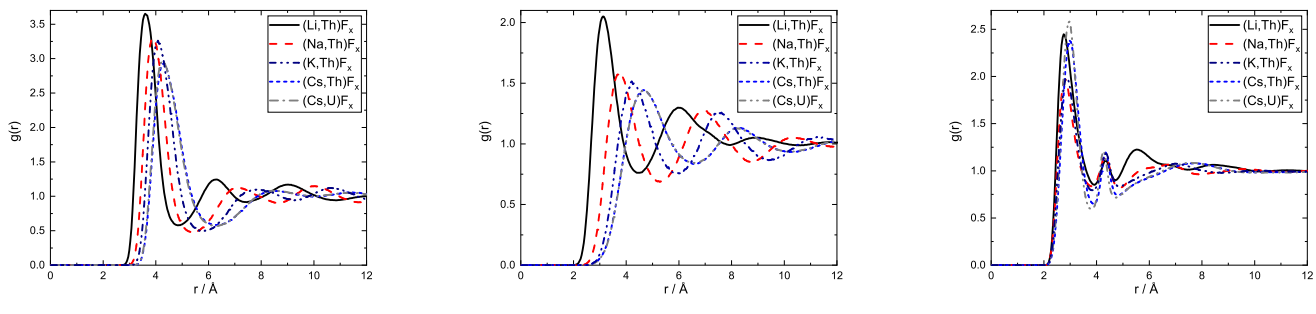
**Table 1** Energies of the Inflection Points and White Lines of  $\text{Th-L}_3$  and  $\text{U-L}_3$  XANES Spectra

sample	inflection point (eV)	white line (eV)
$\text{ThF}_4$	16299.9(5)	16305.3(5)
$\text{ThO}_2$ RT	16300.0(5)	16305.2(5)
$(\text{LiF:ThF}_4) = (0.90:0.10)$	16300.0(5)	16304.9(5)
$(\text{LiF:ThF}_4) = (0.75:0.25)$	16298.9(5)	16304.9(5)
$(\text{LiF:ThF}_4) = (0.50:0.50)$	16300.8(5)	16305.1(5)
$(\text{NaF:ThF}_4) = (0.67:0.33)$	16300.1(5)	16304.9(5)
$(\text{NaF:ThF}_4) = (0.50:0.50)$	16299.1(5)	16304.9(5)
$(\text{NaF:ThF}_4) = (0.33:0.67)$	16300.7(5)	16305.1(5)
$(\text{KF:ThF}_4) = (0.833:0.167)$	16298.5(5)	16304.7(5)
$(\text{KF:ThF}_4) = (0.50:0.50)$	16301.0(5)	16305.6(5)
$(\text{KF:ThF}_4) = (0.33:0.67)$	16300.9(5)	16305.0(5)
$(\text{CsF:ThF}_4) = (0.75:0.25)$	16301.2(5)	16305.1(5)
$(\text{CsF:ThF}_4) = (0.50:0.50)$	16302.1(5)	16306.1(5)
$\text{UF}_4$ RT	17169.6(5)	17174.6(5)
$\text{UO}_2$ RT	17170(5)	17175.8(5)
$\text{UF}_4$	17170.4(5)	17176.3(5)
$(\text{NaF:UF}_4) = (0.50:0.50)$	17171.5(5)	17177.0(5)
$(\text{NaF:UF}_4) = (0.33:0.67)$	17170.5(5)	17176.1(5)
$(\text{KF:UF}_4) = (0.50:0.50)$	17170.7(5)	17176.5(5)
$(\text{KF:UF}_4) = (0.33:0.67)$	17171.2(5)	17176.2(5)
$(\text{CsF:UF}_4) = (0.75:0.25)$	17171.2(5)	17176.1(5)
$(\text{CsF:UF}_4) = (0.50:0.50)$	17171.2(5)	17176.1(5)
$(\text{CsF:UF}_4) = (0.33:0.67)$	17170.9(5)	17175.7(5)
Comparison with samples of Kegler et al. <sup>2</sup> ( $\text{UO}_2$ , schoepite) and Böhler et al. <sup>3</sup> ( $\text{U}_3\text{O}_8$ ), RT.		
$\text{UO}_2$	17169.3(5)	17177.72(5)
schoepite	17175.5(5)	17179.73(5)
$\text{U}_3\text{O}_8$	17171.7(5)	17180.9(5)

Samples are at high temperature, unless otherwise labeled with room temperature (RT).

## Notes and references

- A. L. Smith, M. N. Verleg, J. Vlieland, D. d. Haas, J. A. Ocadiz-Flores, P. Martin, J. Rothe, K. Dardenne, M. Salanne, A. E. Gheribi et al., *Journal of synchrotron radiation*, 2019, **26**, 124–136.
- P. Kegler, F. Pointurier, J. Rothe, K. Dardenne, T. Vitova, A. Beck, S. Hammerich, S. Potts, A.-L. Faure, M. Klinkenberg et al., *MRS advances*, 2021, 1–6.
- R. Böhler, M. Welland, D. Prieur, P. Cakir, T. Vitova, T. Pruessmann, I. Pidchenko, C. Hennig, C. Gueneau, R. Konings and D. Manara, *Journal of Nuclear Materials*, 2014, **448**, 330–339.

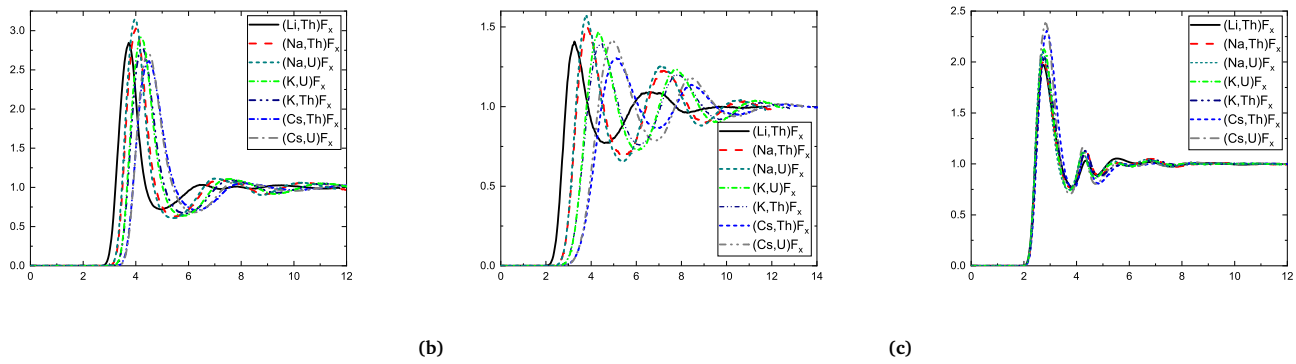


(a)

(b)

(c)

**Fig. 13** Radial distribution functions: (a) An-A, (b) A-A, and (c) F-F in the AF-AnF<sub>4</sub> melts at composition X(AnF<sub>4</sub>) = 0.25 (Li and Cs-based melts) and X(AnF<sub>4</sub>) = 0.33 (Na and K-based melts).

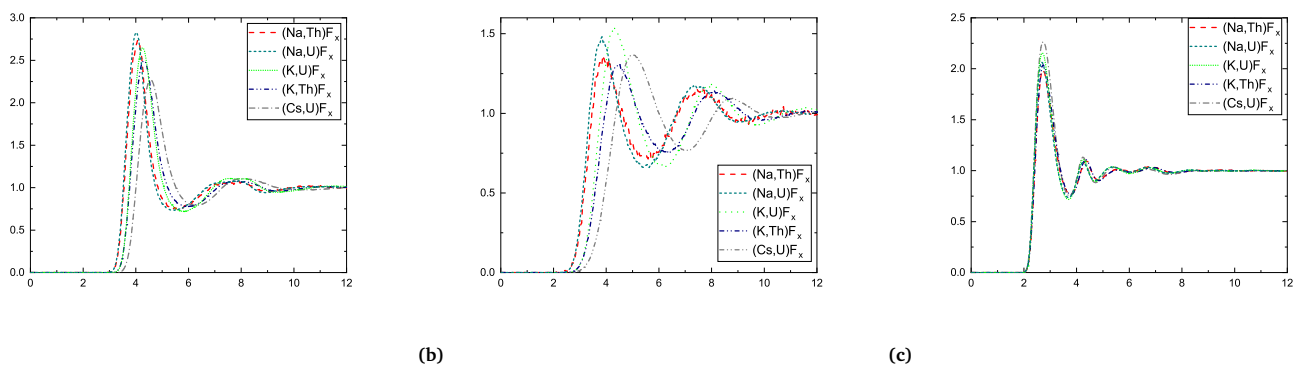


(a)

(b)

(c)

**Fig. 14** Radial distribution functions: (a) An-A, (b) A-A, and (c) F-F in the AF-AnF<sub>4</sub> melts at composition X(AnF<sub>4</sub>) = 0.50.



(a)

(b)

(c)

**Fig. 15** Radial distribution functions: (a) An-A, (b) A-A, and (c) F-F in the AF-AnF<sub>4</sub> melts at composition X(AnF<sub>4</sub>) = 0.67.